Highlights Of RPI Sounding Of The Plasmasphere And Polar Regions At Frequencies In The Whistler And Z-Mode Domains

D. L Carpenter

Space, Telecommunications and Radioscience Laboratory
Stanford University, Stanford, CA 94305

Abstract. The operating frequency of the Radio Plasma Imager (RPI) instrument on the IMAGE satellite extended from 3 kHz to 3 MHz. This wide range made possible conventional free-space O and X mode sounding from locations as distant as 7 Earth radii, while also making possible wave injection in the whistler-mode and Z-mode domains at altitudes less than ≈ 10,000 km. We briefly review three examples of successful work in the latter two domains: (i) upward Z-mode probing along geomagnetic field lines just above the Z-mode cutoff frequency; (ii) downward probing into the ionosphere using whistler-mode waves that undergo two fundamentally different types of reflection; (iii) strong coupling of RPI pulses to the proton plasma in the vicinity of the spacecraft, leading to a new resonance and echoes at multiples of the local proton gyro period.

Keywords: Z-mode sounding, whistler-mode sounding, proton cyclotron echoes, antenna sheath
PACS: 94.05Jq, 94.20Tt, 94.30cv, 94.30Tz

INTRODUCTION

When the RPI instrument [1] on the IMAGE satellite [2] operates at altitudes above ≈ 20,000 km, its entire frequency range from 3 kHz to 3 MHz may be used for sounding with the free space O and X wave modes. However, as the satellite moves to lower altitudes, some part of its operating frequency range becomes usable for whistler-mode and Z-mode probing, and thus provides potential for a new approach to study of the plasmasphere and polar regions at altitudes less than ≈ 10,000 km. In response to this opportunity, new probing tools have been developed that complement the operation of RPI at higher frequencies as a conventional sounder. In this paper we discuss three of the new methods and the problems to which they may be applied. The three topics are: upward sounding using Z-mode waves [3]; whistler-mode sounding of the topside ionosphere at altitudes where key transitions in ion composition take place [4]; stimulation of proton cyclotron echoes in the immediate vicinity of the satellite [5]. For more detailed information on each of these topics, the reader is referred to the indicated references..

Z-MODE SOUNDING

Since plasma parameters such as the electron plasma frequency f_{pe} and electron gyrofrequency f_{ce} are known to decrease monotonically with altitude above the peak of the ionospheric F layer, one might therefore expect the critical frequencies for radio propagation such as cutoffs and resonances to do the same. This is not true, however, for the special case of the cutoff frequency f_Z for Z-mode propagation in a cold plasma, which is given by:

$$f_Z = (f_{ce}/2)\left[-1+\left(1+4(f_{pe}/f_{ce})^2\right)^{1/2}\right] \quad (1)$$

In an altitude range extending from ≈ 1500 km to points above 5000 km, a Z-mode propagation "cavity" regularly exists over a wide range of latitudes. Waves originating at frequencies "within" the cavity can be reflected back toward the origin from reflection points both above and below the wave source. This occurs in spite of the fact that the higher altitude reflection takes place in a plasma region less dense than the one at the source.

CP974, *Radio Sounding and Plasma Physics*
edited by P. Song, J. Foster, M. Mendillo, and D. Bilitza

Figure 1 illustrates the cavity effect by altitude profiles of two frequencies, f_Z and f_{uh} (the upper hybrid resonance), which locally delimit Z-mode propagation in a cold plasma, Also plotted versus distance in geocentric earth radii are models of the plasma parameters f_{ce} and f_{pe}. The left-hand diagram, adapted from [6], was used in a study of natural wave activity in the auroral region, while the right-hand diagram, from [3], represents conditions encountered by RPI during sounding operations at middle latitudes.

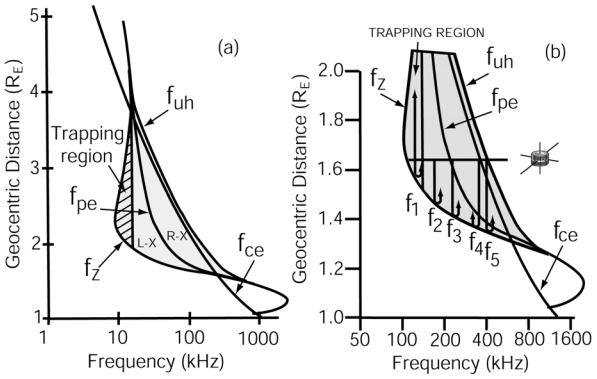

FIGURE 1. (a) Model plot, adapted from [6], of the variation of key plasma parameters with geocentric distance along polar region field lines, showing by shading the Z-mode propagation cavity or trapping region, (b) Modified version of Fig.1a illustrating a number of idealized ray paths for Z-mode echoes in a particular case of sounding by RPI near L = 3 in the plasmasphere..

It is clear that the curve for f_Z undergoes a minimum with altitude and that the minimum is reached within an altitude range in the topside ionosphere where the ratio f_{pe}/ f_{ce} falls to a minimum value. In Fig, 1a, hatching shows at each altitude a range of frequencies for which locally launched waves could be expected to return after reflection from points both above and below the source.

Figure 1b shows schematically the propagation paths of a sequence of waves launched by RPI over a range of frequencies from f_Z to f_{uh}. Waves at frequency f_1, just above f_Z, remain within the cavity and are reflected from both above and below RPI. In contrast, frequencies f_2, f_3, and f_4 exceed the upper frequency limit of the cavity and the corresponding waves reflect only at points below the spacecraft.

Two examples of propagation within a cavity are illustrated in Fig. 2 on plasmagrams showing echo intensity in coordinates of virtual range (echo range at an assumed propagation velocity of c) versus transmitted frequency. Range is plotted from 0 to 4.0 Earth radii and frequency from 350 kHz to 480 kHz. On both records there is a band of no electromagnetic propagation at the lower frequencies, followed by a broad belt of noise that is attributed. to a combination of scattering of RPI Z-mode pulses from irregularities [7,8] as well as Z-mode noise from distant sources [9,10]. The local Z-mode cutoff f_Z is found to be at or near the low-frequency edge of this band. Clearly outlined against the background noise are patterns of discrete echo traces that begin at f_Z.

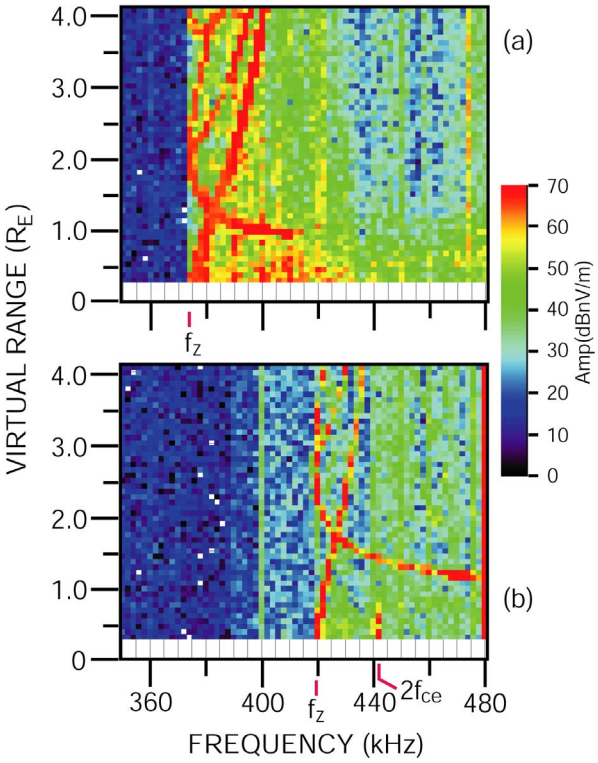

FIGURE 2. RPI plasmagrams from 28 July 2001 showing multicomponent Z-mode echoes detected within the plasmasphere on successive soundings 2 ½ min apart.

An interpretation of the propagation paths of the discrete echoes shown in Fig. 2a is presented in Fig. 3. Above is a rescaled tracing of the observed echo pattern in Figure 2a, while the diagram below shows on the same frequency scale the variation with altitude of f_Z in a postulated propagation cavity. The sounding is assumed to have taken place at an altitude above the minimum value of f_Z in the cavity. The upward and downward directions of propagation are identified as D and C, respectively. As the sounder frequency steps upward and reaches f_Z at ≈ 372 kHz, an echo f_i is received from a reflection altitude below IMAGE, forming the first elements of what becomes the down-sloping C echo trace. As the sounder continues above f_Z, echoes such as f_j begin to return from both higher and lower altitudes. The D echo forms near zero range and extends rapidly toward longer delays because of the small spatial gradients in f_Z encountered in the upward direction. Finally, the sounder frequency

exceeds the peak value reached by the f_Z profile above IMAGE, after which echoes such as f_k can return from below only..

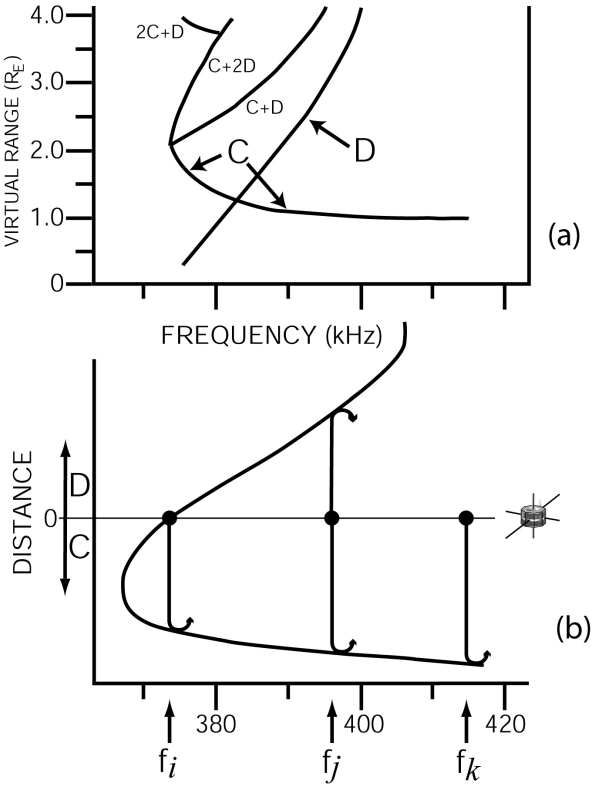

FIGURE 3. Interpretive model of the echoes of Fig. 2a for the case of a sounder location above the minimum in Z-mode cutoff frequency with altitude. The horizontal scale has been expanded by a factor of ≈ 2 to facilitate comparisons of echo delays.

.

The remarkable clarity of the echo traces suggests that the signals involved were guided or ducted by geomagnetic field-aligned irregularities, a phenomenon that since 1956 has been found necessary to explain ground-observed whistler-mode signals [11,12]. Ducting has recently been invoked to explain discrete O and X mode propagation from RPI [13,14] and was earlier identified from observations with ISIS-series satellites [15,16]. The existence of a single discrete propagation path passing through the satellite position is indicated by the additional components in Fig. 2a marked C + D, C + 2D, and 2C +D. Each of the higher order components consists of some combination of the measured delays along the original C and D paths.

When RPI launches Z-mode waves from an altitude below the minimum of a Z-mode cavity, a quite different echo pattern is detected, but again there are well defined echo components from upward and downward directions as well as combinations of the two in the manner of Fig. 3a. Thus it was concluded that an explanation of events such as that of Fig. 2a requires the existence of both a propagation cavity as well as the occurrence of ducted propagation along the magnetic field [3]..

Diagnostic Uses of Z-Mode Upward Probing

The propagation cavity is of geophysical interest for a number of reasons. In the case of the D component in Fig. 2a, representing upward propagation along the geomagnetic field from IMAGE, an inversion technique can be applied to determine the electron density profile along the path up to the altitude limit reached by the measured D component (for the conditions of Fig. 1a, that limit was predicted to be ≈ 4 R_E). The inversion method, developed by T.F. Bell of Stanford University and described in [3], was applied in the case of Figure 2a with the results shown in Fig. 4 on a plot of plasma density versus magnetic latitude for L=2.1 and 2.3.

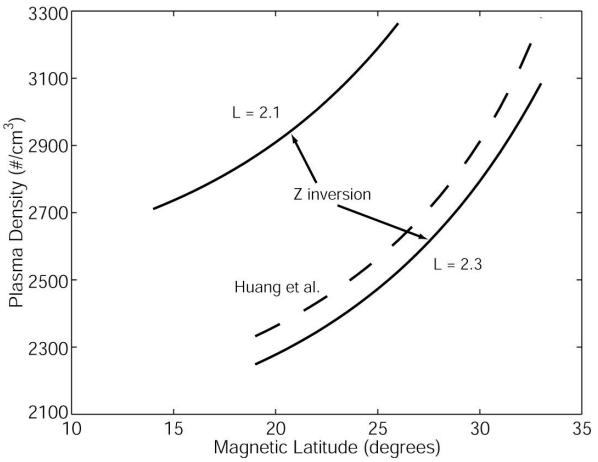

FIGURE 4. Plots of electron density versus magnetic latitude at two L values, 2.1 and 2.3, inferred from the upward propagating Z-mode signals illustrated in Figs. 2a and 2b and identified as component "D" in Fig. 3. The dashed curve is for L = 2.3 from the Huang et al. [17] model for a different date. That model is based upon inversion of free-space mode echoes that propagated to RPI along multiple field aligned paths.

Density is shown from the position of IMAGE upward to a point ≈ 5000 km above IMAGE along $\mathbf{B_0}$. For comparison we show a profile for L ≈ 2.3 obtained for another date by Huang et al. [17] using an inversion of the X mode trace for propagation downward from the satellite. The Huang et al profile was scaled by a factor of 0.8, but there is excellent agreement on the shape of the curve between the downward (X-mode) and upward (Z-mode) analyses.

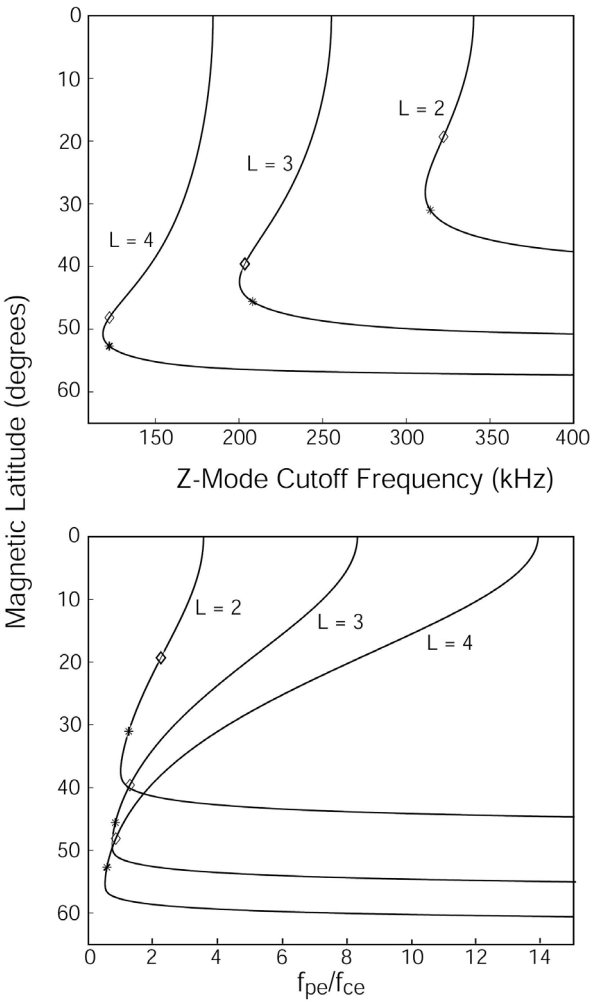

FIGURE 5. (a) Plot of calculated Z-mode cutoff frequency f_Z versus magnetic latitude along geomagnetic field lines at L = 2,3, and 4, illustrating the widespread occurrence of a low-altitude minimum in f_Z within the plasmasphere. A dipole magnetic field model and a diffusive equilibrium density model were assumed. Altitudes of 3000 and 5000 km are marked. (b) Corresponding plot of the ratio f_{pe}/ f_{ce} along the field lines.

The f_Z profile with altitude may be used as a diagnostic of plasma composition along $\mathbf{B_o}$ in the topside ionosphere region. If one assumes a three-component plasma in diffusive equilibrium above a reference altitude, a small positive electron temperature gradient along $\mathbf{B_o}$, and a known value of electron density at the magnetic equator, one then finds that in order to place a minimum in the f_Z profile in the 3000-5000 km altitude range where it has been observed, there are important constraints on the relative ion composition at the reference level.

Figure 5a is a plot of calculated f_Z profiles along $\mathbf{B_o}$ at three L values, 2,3, and 4, with magnetic latitude plotted on the vertical scale. In Fig. 5b are shown corresponding plots for the ratio of f_{pe}/ f_{ce}. Marks along the curves show the locations of the 3000 km and 5000 km altitudes, respectively. Using the empirical model of electron density at the equator of [18], an assumed ratio of He^+ to H^+ of 0.05 to 0.1 at the equator, an assumed value of 2 for the ratio of T_e at the equator to T_e at the 1000 km reference level, it was found that a distribution of 82% O^+, 17% He^+ and 1% H+ at the reference level would predict the profiles of Fig. 5, which exhibit an f_Z minimum in the observed 3000-5000 km altitude range [3]. The altitude of the minimum appeared to be sensitive to the choice of composition at the reference level, thus suggesting that further observations of this kind could be used to investigate the poorly known distribution of ions in the coupling region between the ionosphere and the plasmasphere.

Z-mode probing of the kind described here has only recently been developed [3]. With further refinement, it can become a valuable adjunct to conventional radio sounding. The RPI data offer many opportunities for application of the new method. For example, many well defined Z-mode echoing events have been detected in the plasmapause region, or plasmasphere boundary layer (PBL) [19], where little is known of the variations of the plasma properties along the field lines at low altitudes.

WHISTLER-MODE SOUNDING OF ALTITUDES < 4000 KM

A new whistler-mode tool for probing the topside ionosphere has recently been reported [4]. Pending publication of a full description of the method, we limit ourselves to a simple outline of the phenomena involved and their apparent diagnostic potential.

"MR" Whistler-Mode Echoes

When the RPI operates below ≈ 4000 km altitude at frequencies as low as 6 kHz, the plasmagrams regularly contain echoes that result from so-called "magnetospheric reflections" (MRs) at locations where the wave frequency matches the local lower hybrid resonance frequency f_{lh} [20,21]. These echoes appear in discrete and diffuse spectral forms. The discrete MR form tends to exhibit a nose-like shape on plasmagrams because of extended time delays at the form's minimum and maximum frequencies. Those limiting frequencies, usually separated by a few kHz, are associated, respectively, with f_{lh} at the location of the satellite (the lower frequency), often near 6 kHz, and the maximum value of f_{lh} along the field line extending earthward from IMAGE (the upper frequency), often near 12 kHz. The diffuse MR spectral form frequently exhibits upper and lower frequency limits similar to those of the discrete forms, but may occur without such clear limits. The key formative elements in the MR echo phenomenon appear to be: (1) propagation of RPI whistler-mode waves at high wave normal angles, near the so called resonance cone around the direction of the magnetic

field; (2) reflection of the waves near a point where the wave frequency matches the local f_{lh}; (3) in the case of the diffuse echoes, scattering of the waves in the presence of field aligned irregularities such that the echoes reach the satellite with varying time delays.

Of special interest with these "MR" whistlers, is the fact that the received echo signal provides a measure of the f_{lh} at two points along a field line and thus can provide information on m_{eff}, the "effective mass" of the plasma in the important transition region between the O^+ dominated lower ionosphere and the eventually H^+ dominated region at higher altitudes. This can be seen from the following expression for f_{lh}:

$$\frac{1}{m_{eff}\left(m_p/m_e f_{lh}^2\right)} = \frac{1}{f_{pe}^2} + \frac{1}{f_{ce}^2} \qquad (2)$$

where m_p/m_e is the proton/electron mass ratio, f_{pe} and f_{ce} are the electron plasma and gyrofrequencies, respectively, and

$$\frac{1}{m_{eff}} = \frac{\alpha}{1} + \frac{\beta}{4} + \frac{\gamma}{16} \qquad (3)$$

where α, β, and γ are, respectively, the fractional abundances of H^+, He^+, and O^+. It is clear that within altitude ranges over which the r.h.s of (2) does not change appreciably, the value of f_{lh} will be sensitive to changes in m_{eff} (by as much as a factor of 16) associated with altitude variations in ion composition.

Bottom-side Ionosphere Whistler Mode Echoes

RPI soundings at whistler mode frequencies regularly exhibit echoes that extend over a wide range of frequencies and are interpreted as having reflected from the steep density gradients at the bottom side of the ionosphere [8]. Such echoes often accompany the MR whistler mentioned above. Since they provide an integral measure of the electron density between IMAGE, say at ≈ 3000 km, and the ionosphere at ≈ 100 km, the information they provide may be used to constrain the density/plasma composition model that is found most consistent with the MR event on the same record.

The RPI data set contains many examples of MR whistler echoes as well as bottom-side ionosphere echoes.. New analysis tools for use with these phenomena have been developed only recently [4], but now can be applied to a large volume of RPI data.

PROTON CYCLOTRON ECHOES

At altitudes ranging from ≈ 1500 km to 20,000 km in the plasmasphere, the RPI instrument on IMAGE can couple strongly to protons in the immediate vicinity of the satellite as it transmits 3.2-ms pulses and scans from 6 to 63 kHz or 20 to 326 kHz [5]. Those soundings also give rise to a new resonance at a frequency ≈ 15% above the electron cyclotron frequency f_{ce} [5]. The coupling to protons is revealed in echoes that arrive at multiples of the local proton cyclotron period t_p. Lower-altitude (< 4,000 km) versions of several of these proton cyclotron (PC) echo forms were observed in the topside ionosphere by sounders in the ISIS satellite era, among them discrete echoes in the whistler-mode domain below f_{ce} and in the nominally non-electromagnetically propagating domain above f_{ce} [22,23,24]. Also seen on ISIS satellites were spur-like broadenings of resonances such as the one at the electron plasma frequency f_{pe} [25,26,22].

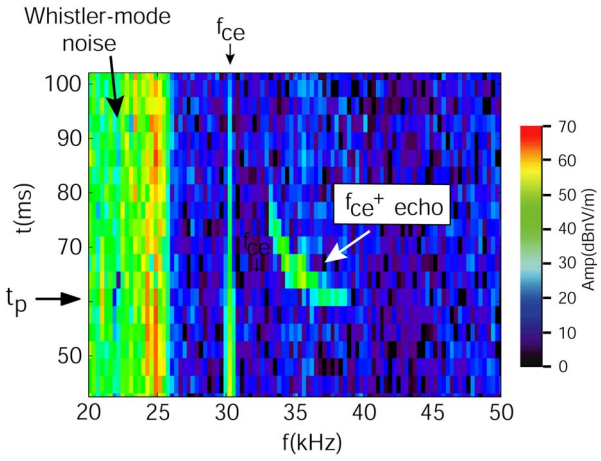

FIGURE 6. Portion of an RPI plasmagram showing a well defined proton cyclotron echo that exhibits extended delays at frequencies just above f_{ce} and then approaches a constant delay at the local value of the proton gyro period t_p.

The f_{ce}^+ Echo

Figure 6 shows an example of what has been called an f_{ce}^+ echo, a phenomenon often observed in the plasmasphere by RPI at frequencies from ~10 to 20% above f_{ce} [5]. The plasmagram presents time delay from ≈ 40 to 100 ms versus frequency from 20 to 50 kHz. IMAGE was at L ≈ 3.7, well inside an extended plasmasphere at an altitude of ≈ 14,000 km and in the mid-afternoon sector. The local electron density was ≈ 560 el-cm^{-3}. The sounding format involved single 3.2-ms pulses transmitted at 250-ms intervals as frequency was increased in steps of 300 Hz from 6 kHz to 63 kHz.

On Fig. 6 the local value of f_{ce} is well defined at ≈ 30.3 kHz by a resonance spike, a type of response that is regularly present on sounder records from the topside ionosphere [27 and references cited therein]. A band of whistler-mode noise extends upward in frequency to a relatively sharp cutoff at ≈ 26 kHz. This band is attributed to multi-path propagation and scattering of a variety of whistler-mode signals, including naturally occurring wave emissions, whistler-mode emissions triggered by lightning, and multiple whistler-mode signals from ground-based transmitters. In the figure, the f_{ce}^{+} echo first appears at ≈ 33.3 kHz, ≈ 3 kHz above f_{ce} in frequency, and extends to 39 kHz. It exhibits a time-delay-versus-frequency form something like that of a hockey stick, at first falling steeply in delay with increasing frequency and then curving to reach a constant delay of ≈ 61 ms. That delay corresponds closely to the local proton cyclotron period $t_p = 1836/f_{ce}$.

On IMAGE the occurrence rates of PC echoes above f_{ce} were highest during periods when the angle φ between the spacecraft velocity vector $\mathbf{V_S}$ and the geomagnetic field $\mathbf{B_o}$ was small, near 20°, but on occasion such echoes were detected when φ approached 90°.

The f_{ce}^{+} Resonance

A new phenomenon, called the f_{ce}^{+} resonance, has been observed at a frequency ≈ 15% above f_{ce} [5]. This resonance is apparently confined to altitudes above ≈ 7,000 km. It is illustrated by the plasmagram of Fig. 7, which displays time delay from 0 to 178 ms versus frequency from 6 to 63 kHz. At the time of the figure, IMAGE was at L ≈ 3.6 and at an altitude of ≈ 12,000 km, well inside the plasmasphere. Three echo forms appear, a WM echo (see explanation below), multiple f_{ce}^{+} echoes, and an f_{ce}^{+} resonance. The WM echo, extending from ≈ 9 to 17 kHz at a constant delay of ≈ 45 ms, appears as a discrete intensity enhancement within the usual whistler-mode noise background. The value of f_{ce} is well marked by a tapered resonance spike at ≈ 42 kHz. Approximately 3 kHz above f_{ce}^{+} is an "f_{ce}^{+} resonance." This resonance differs from the spike at f_{ce} in that it extends to the top of the record and (in this case) is not clearly defined in the first ≈ 30 ms after the beginning of the transmitter pulse. Along the high-frequency side of the f_{ce}^{+} resonance are f_{ce}^{+} echoes that arrived at multiples of t_p, the first at ≈ 44.5 ms, the second at ≈ 89 ms, and the third at ≈ 133 ms.

There are differences in amplitude among the echo forms illustrated in Fig. 3: portions of the WM echo near 10 kHz are ≈ 10-15 dB stronger than the f_{ce}^{+} resonance or f_{ce}^{+} echoes.

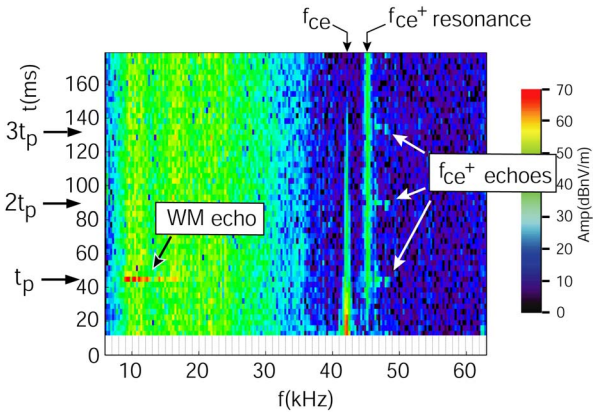

FIGURE 7. RPI plasmagram illustrating three effects, a proton cyclotron echo in the whistler-mode domain (WM), a resonance at a frequency just above the electron gyro resonance f_{ce}, and discrete echoes at multiples of t_p

WM Echoes

Of special interest are exceptionally strong echoes in the whistler-mode domain near 10 kHz called WM echoes [5]. On a given orbit, these invariably appeared at altitudes near 5,000 km and below and could be detected at altitudes up to ≈ 12,000 km. In some cases, the echoes appeared on plasmagrams showing other PC echo activity, as illustrated in Fig. 7.

Most of the WM echoes observed thus far were found within the plasmasphere or the PBL at magnetic latitudes between -60° and 60°. They were evident on occasion at higher latitudes and over the polar regions, but tended to be obscured there by strong natural whistler-mode noise with power spectral density 10 dB or more above the noise levels in the plasmasphere. Samplings showed strong WM echo activity at several widely spaced magnetic local times, suggesting that such echoes may occur in all local time sectors.

At each frequency during a given sounding, WM echoes tended to repeat at time delays that were multiples of t_p. Figs. 8a to 8c display such effects on plasmagrams recorded on three different orbits at altitudes ≈ 10,700 km, ≈ 7,700 km, and ≈ 4,200 km, respectively. As altitude decreased, the inter-echo time delay decreased accordingly.

In the stronger magnetic fields below ≈ 3,000 km altitude, the time interval at each frequency between successive high-order echoes fell below 6.4 ms, the minimum interval allowing separation of echoes by one 3.2-ms time-delay pixel, and individual echoes could no longer be resolved. In such cases, the echoes formed a "continuous" response extending to multiple values of t_p..

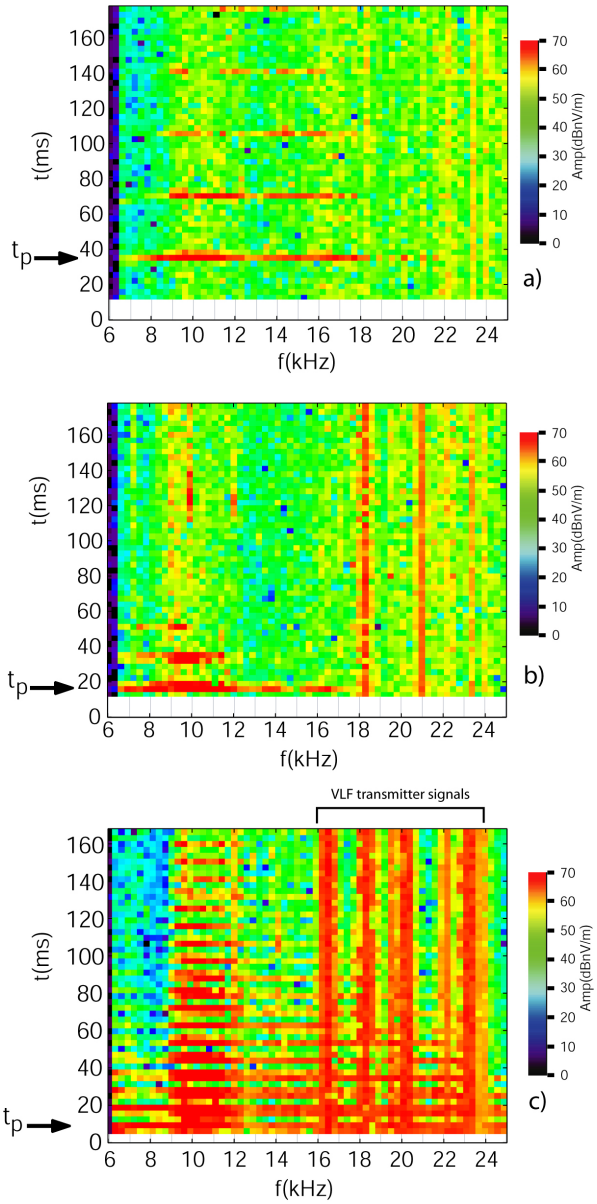

FIGURE 8. RPI plasmagrams showing proton cyclotron echoes in the whistler-mode domain, repeating at multiples of the local proton gyro period t_p. The examples were recorded on three different orbits at altitudes 10,700 km (a), 7700 km (b), and 4200 km (c). The vertical lines between 16 and 24 kHz in (c) represent whistler-mode transmissions from ground transmitters.

When the angle φ was near a local minimum of order 10°, WM echoes were observed to repeat at multiples of t_p up to 15 or more. The data indicate that WM echo detection near 10 kHz was largely confined to a region of radius ≈ 300 m around the field line of excitation, and that the peak excitation of the protons occurred as a transient event at the beginning of each *rf* pulse.

Comments On Physical Mechanisms Of PC Echoes

The authors of [5] suggest that PC echoes and the new resonance are driven by a variety of mechanisms, but discuss only the WM category in detail.

Time delay measurements of WM echoes near 10 kHz indicated that the energization of the protons by a given 3.2-ms sounder pulse was essentially a transient process that occurred at the beginning of the pulse, and to that extent did not involve replication of the pulse *rf* frequency by the echo. It was concluded that the WM echo mechanism is quasi-electrostatic in nature, with spatial bunching of protons during the first positive *rf* half cycle on one of the antenna elements, such that a high voltage is induced in the RPI antenna at multiples of t_p after $t = 0$ following the leading edge of the transmitter pulse.

Most WM echoes were observed when IMAGE moved at low angles to $\mathbf{B_0}$ and was within a distance of ≈ 300 m transverse to the field line of original excitation of the plasma. The echoes showed no measurable whistler-mode propagation delay from a source, which is consistent with the inferred electrostatic nature of the echoes and the closeness of the antenna to the source field lines.

The high intensity of the lower-order WM echoes, which regularly saturated the RPI receiver near 10 kHz, as well as the lack of detectable WM echo activity above 12,000 km altitude, were attributed in part to the fact that proton energization at the leading edge of the sounder pulse was at maximum levels when the *rf* of the pulse was below, but near, the local proton plasma frequency $f_{pp} = f_{pe}/43$. f_{pp} reaches a maximum of ≈ 13 kHz at the lower IMAGE altitudes, but falls below 6 kHz (the lowest sounder operating frequency) above 12,000 km.

In contrast to WM echoes, f_{ce}^+ echoes occurred at frequencies well above f_{pp} and were thus outside the range where significant transient energization was expected. Also in contrast to WM echoes, f_{ce}^+ echoes appeared to replicate the sounder pulse frequency and in so doing experienced large frequency-dependent increases in travel time as f_{ce} was approached from above. This dispersion as well as a year-to-year decrease in f_{ce}^+ echo activity with increasing separation of the antenna from the "excited" field lines, is consistent with an explanation of f_{ce}^+ echoes observed in the ISIS series in terms of thermal-mode propagation from a perturbed proton distribution [24]. A possible source of energy for the comparatively weak f_{ce}^+ echoes is the quasi-static electric field that exists in the ion sheath that surrounds each antenna element in the immediate aftermath of an *rf* pulse, as discussed in [5].

The new resonance above f_{ce} suggested the existence of a ringing phenomenon in the plasma that is unique to altitudes above ≈ 7,000 km. The resonance mechanism appears to operate independently of the f_{ce}^{+} echo mechanism, although both phenomena were found within a similar range of frequencies above f_{ce}. The long enduring nature of the resonances, lasting at times for at least 300 ms, suggests that the perturbed plasma environment in which the ringing occurred was carried with the spacecraft a kilometer or more beyond the ≈ 300 m transverse distance within which the WM echoes were found. The collapse of the ion sheath following an *rf* pulse may provide energy for the ringing process. This collapse may on occasion delay the onset of the detected resonance, in the manner proposed in [28], where it was argued that in the case of certain ionospheric resonances, the antenna sheath may temporarily exclude very short wavelength stimulated waves.

Previously suggested processes that were considered relevant to PC echoes above f_{ce} and to the new resonance include: (i) coupling between an excited Z-mode wave and longitudinal plasma waves [26]; (ii) the accumulation of negative charge on an electric antenna during an *rf* pulse [23], and (iii) Bernstein-mode propagation to an antenna from an excited proton population [24].

There is much more to learn about proton cyclotron echoes and the high altitude f_{ce}^{+} resonance, both from existing data and future experiments. A variety of mechanisms appear to be at work, only a few of which have been considered here.

CONCLUDING REMARKS

In addition to its success as a high altitude sounder using free space O and X mode waves and also scans of natural wave activity, the RPI instrument on IMAGE has provided a platform for development of several powerful new methods of probing at frequencies in the whistler and Z-mode domains. These methods, currently in early stages of development and application, have shown several ways in which new information can be obtained about plasma density, wave ducting, and plasma composition in the important altitude range linking the Earth's regular ionosphere with the overlying regions.

ACKNOWLEDGMENTS

The work reviewed here was supported by NASA under: (i) a subcontract from Southwest Research Institute to U. Mass. Lowell, (ii) a subcontract from U. Mass. Lowell to Stanford University, (iii) a guest investigator grant to V. Sonwalkar at U. Alaska Fairbanks. Much credit for the three studies reviewed is owed to the coauthors listed in references [3,4,5] listed below. T. F. Bell is responsible for the bulk of the theoretical work represented in the sections on Z-mode probing and PC echoes. Don Muldrew is to be thanked for his careful reading of and comments upon reference [5].

REFERENCES

1. B. W. Reinisch et al., *Space Sci. R*ev. **91**, 319-359 (2000)..
2. J. L. Burch, *Space Sci. R*ev. **91**, 1-14 (2000).
3. D. L. Carpenter et al., *J. Geophys. Res*. **108**(A12), 1421, doi:10,1029/2003JA010025 (2003).
4. V. S. Sonwalkar et al., "Observations of Magneto-spherically Reflected (MR) Whistler Mode (WM) Echoes Observed by Radio Plasma Imager (RPI) on the IMAGE satellite: Diagnostics of Electron Density and Ion Composition," AGU Fall Meeting 2006, abstract #SM11B-0323.
5. D. L. Carpenter et al., *J. Geophys. Res*. **112,** A08208, doi:10,1029/2006JA012139 (2007).
6. D. A. Gurnett et al., *J. Geophys. Res*. **88,** 329-340 (1983).
7. D. G. Muldrew, *Proc. IEEE*, **57**, 1097-1107 (1969).
8. V. S. Sonwalkar et al., *J. Geophys. Res*. **109,** A11212, doi:10,1029/2004JA01047 (2004)
9. R. F. Benson and H. K. Wong, *J. Geophys. Res*. **92,** 1218-1230 (1987).
10. R. F. Benson, "Elusive Upper Hybrid Waves in the Auroral Topside Ionosphere" in *Auroral Plasma Dynamics, Geophys. Monogr. Ser. Vol. 80*, edited by R. Lysak, AGU, Washington, D.C., 1993, pp.
11. R. L. Smith, *J. Geophys. Res*. **66,** 3699-3707 (1961).
12. R. A. Helliwell, *Whistlers and Related Ionospheric Phenomena*, Stanford University Press, Stanford CA, 1965, pp. 43-55.
13. B. W. Reinisch et al., *Geophys. Res. Lett*. **28**, 4521-4524 (2001).
14. S. F. Fung et al., *Geophys. Res. Lett*. **30**(11), 1589, doi:10,1029/2002GL016531 (2003).
15. D. B. Muldrew, *J. Geophys. Res*. **68,** 5355-5370 (1963).
16. B. T. Loftus et al., *Ann. Geophys*. **22**, 530-538 (1966).
17. X. B. Huang et al., *Adv. Space Res*. **33**, 6, 829-832 (2004).
18. D. L. Carpenter and R. R. Anderson, *J. Geophys. Res*. **97,** 1097-1108 (1992)
19. D. L. Carpenter and J. Lemaire, *Ann. Geophys*. **22**, 4291-4298 (2004).
20. I. Kimura, *Radio Science* **1**, 269-283 (1966).
21. R. L. Smith and J. J. Angerami, *J. Geophys. Res*. **73,** 1-20 (1968).
22. R. E. Horita, *Radio Science* **22**, 671-686 (1987).
23. H. Oya, *J. Geophys. Res*. **83,** 1991-2008 (1978).
24. D. M. Muldrew, *Radio Science* **33**, 1395-1411 (1998).
25. J. W. King and D. W. Preece, *J. Atmos. Terr. Phys*. **29**, 1387-1390 (1967).
26. R. F. Benson, *Radio Science* **10**, 173-185 (1975).
27. R. F. Benson, *Radio Science* **12**, 861-878 (1977).
28. D. B. Muldrew, *J. Geophys. Res*. **77,** 1794-1801 (1972).